A Zonally Averaged Ocean Model for the Thermohaline Circulation. Part II: Interocean Circulation in the Pacific–Atlantic Basin System

THOMAS F. STOCKER AND DANIEL G. WRIGHT*

Centre for Climate and Global Change Research, Department of Meteorology, McGill University, Montreal, Quebec, Canada

(Manuscript received 4 September 1990, in final form 10 April 1991)

ABSTRACT

The zonally averaged, latitude–depth ocean model, developed in Part I, is extended to a two-basin system representing the Atlantic and Pacific. Steady states are calculated under two different surface boundary conditions to study a possible global thermohaline circulation linking the Pacific and the Atlantic. If the surface temperature and salinity profiles are identical functions of latitude in both the Pacific and the Atlantic, the steady state under restoring boundary conditions consists, in spite of the different basin extensions, of a two-cell structure in each basin. Upon switching to mixed boundary conditions the state is unstable, and a one-cell circulation with downwelling at high northern latitudes develops in both basins.

For a realistic surface salinity profile that is fresher in the Pacific, the steady state under restoring boundary conditions is completely different. It exhibits a global thermohaline circulation with strong interocean mass exchange. Deep water is formed primarily in the North Atlantic, from which a deep flow spreads into the Pacific, where it upwells. This state is stable under mixed boundary conditions. The meridional heat flux is to the south in the Pacific and to the north in the Atlantic with maximum values of order 0.7 PW (1 PW = 10^{15} W). Both temperature and salinity structures of the steady state compare favorably with the observed zonal averages. The model also demonstrates that this "conveyor belt" circulation is maintained by net evaporation in the Atlantic and net precipitation in the Pacific.

Two deglaciation experiments simulating the termination of the last ice age are performed by applying a freshwater flux anomaly of 0.12 Sv and 0.06 Sv (1 Sv ≡ 10^6 m^3 s^{-1}) in the North Atlantic. The strong anomaly shuts off the interocean exchange, and deep water is formed subsequently only in the Southern Ocean. For the small anomaly the interocean circulation weakens but remains in operation. When the anomalous flux is switched off, the final equilibrium state for the first experiment is the mode with no interocean exchange, while in the second experiment the state returns to the original conveyor belt. The global thermohaline circulation thus exhibits more than one stable equilibrium under realistic surface forcing.

1. Introduction

Beyond controlling the meridional heat flux in a single ocean basin like the Atlantic, the thermohaline circulation is likely to have a global significance within the climate system. Observations confirm that the main region of deep-water formation is located in the North Atlantic (Warren 1981) with rates estimated at 14 to 20 Sv (1 Sv ≡ 10^6 m^3 s^{-1}), while the Pacific Ocean shows primarily upwelling. Based on an analysis of water characteristics in the main ocean basins, Gordon (1986) proposed that these two areas are linked by a thermocline flow of relatively warm water from the Pacific through the Indian Ocean into the South Atlantic, thus feeding deep-water formation in the North Atlantic. A corresponding deep flow exports Atlantic water to the Indian and Pacific oceans. Such a global thermohaline circulation would connect the three major ocean basins, acting like a conveyor belt for water masses, and would represent a key element of our climate system.

In Part I (Wright and Stocker 1991) we have developed a zonally averaged ocean model and shown qualitative agreement with three-dimensional ocean general circulation models (OGCMs). We are therefore encouraged to apply an extended version of the model to investigate whether the main ocean basins are indeed connected by a global thermohaline circulation. A second purpose of this paper is to study the stability of such a conveyor belt circulation. More specifically, we examine how freshwater released into the Atlantic Ocean during the termination of an ice age affects the global thermohaline circulation.

Support for the idea that the various ocean basins are communicating via a thermohaline flow was recently provided by several three-dimensional OGCM experiments. Cox (1989) studied the steady-state water mass structure of the World Ocean under zonally uni-

* Permanent affiliation: Department of Fisheries and Oceans, Bedford Institute of Oceanography, Dartmouth, Nova Scotia, Canada.

Corresponding author address: Dr. Thomas Stocker, Lamont-Doherty Geological Observatory, Columbia University, Palisades, NY, 10964.

form restoring boundary conditions on both temperature and salinity. When the thermohaline flow was enhanced by adding salt to the North Atlantic, water masses originating from the North Atlantic were identified in the Indian and Pacific oceans. Maier-Reimer and Mikolajewicz (1989) presented results of the global, annual-mean version of the Hamburg OGCM, which was spun up under restoring boundary conditions. From this essentially steady state the salt flux was diagnosed, and integration continued under mixed boundary conditions. The model was able to clearly reproduce a global thermohaline circulation linking the main ocean basins. A highly symmetric two-basin version of the Bryan–Cox OGCM was used by Marotzke and Willebrand (1991) to examine multiple equilibria. The two basins had identical geometry, were symmetrically forced, and were connected by a specified Antarctic Circumpolar Current. Under mixed boundary conditions four stable states could be realized: two conveyor belt circulations and two states for which there was little interocean exchange, and deep water was formed either in high northern or high southern latitudes in both basins.

Modifications in the thermohaline circulation can be an important factor for climatic change. Stommel (1961) found, using a box model, that a perturbation of the thermohaline circulation might cause it to jump into a different mode of operation; stable and unstable equilibria found in several recent ocean models give further support. Broecker et al. (1985) and Broecker and Denton (1989) show evidence of significant changes in deep-water formation rates of the North Atlantic during the termination of the last ice age. Meltwater from the disintegrating North American ice sheets, which flows into the North Atlantic at various latitudes, can influence the thermohaline circulation. The immediate local effect is to stabilize the water column and decrease deep-water formation, which results in a reduced oceanic meridional heat transport. If the global conveyor belt flow suggested by Gordon (1986) is operating, one must expect that a modification of the Atlantic deep circulation will also have a global impact.

The early model studies (Bryan 1986; Marotzke et al. 1988) on the effect of deglaciation on the thermohaline circulation use unrealistic scenarios and consider only one ocean basin. A steady state is perturbed by adding or removing salt at a given time. In a more realistic scenario the surface flux of salt is modified for several thousand model years. This was first done by Maier-Reimer and Mikolajewicz (1989) in their global OGCM. Their results indicate that an anomaly ten times smaller than the current glacial meltwater estimate of about 0.1 Sv is already sufficient to switch off the Atlantic meridional heat transport.

The paper is organized as follows. Section 2 explains the model setup. The steady states that evolve under symmetric surface forcing and their stability are presented in section 3. Section 4 deals with the global thermohaline circulation obtained when realistic surface salinity is used. Two deglaciation experiments are discussed in section 5. Conclusions follow in section 6.

2. Model setup for the Pacific–Atlantic basin system

To simulate the global thermohaline circulation, the ocean model is extended to two basins of 120° and 60° angular width representing the Pacific and Atlantic, respectively. The Pacific basin extends from 55°S to 50°N, the Atlantic from 55°S to 80°N. Meridional overturning transport in the individual basins depends strongly on the zonally averaged east–west pressure gradient. This quantity cannot be determined from the zonally averaged equations and hence must be parameterized. As explained in Part I, we use the parameterization

$$\frac{\Delta p}{\Delta \Lambda} = -2\epsilon s c^2 \frac{\partial p}{\partial s}, \tag{1}$$

where s and c are the sine and cosine of latitude, and $\Delta p/\Delta\Lambda$ and $\partial p/\partial s$ are the zonally averaged zonal and meridional pressure gradient components. In Part I we argued that the value of ϵ depends on the width of the basin. Here we assume that, for a specified north–south density gradient, the density contrast across a wide basin is independent of the width of the basin. Combined with the hydrostatic approximation, this suggests that the pressure difference across the basin is independent of the basin width, so the pressure gradient (and hence ϵ) is inversely proportional to the basin width. This is also consistent with the fact that the zonally averaged east–west velocity comes closer to geostrophy with increasing angular width.

Various runs have shown that $\epsilon = 0.2$ for the Atlantic (and hence $\epsilon = 0.1$ for the Pacific) yields reasonable values of the meridional overturning under realistic surface forcing. Independent analysis of the three-dimensional OGCM (Part I, section 2c) gives $\epsilon = 0.3$ for the Atlantic. Test runs suggest that use of $\epsilon = 0.3$ rather than $\epsilon = 0.2$ would not influence the basic conclusions drawn here.

The Southern Ocean region plays an important role, since all interbasin exchange in the model occurs through it. An important assumption made here is that the temperature and salinity may be approximated as zonally uniform within this region, so that the Southern Ocean can be modeled by cells that extend 360° longitudinally. In reality, the Antarctic Circumpolar Current continuously spreads the influence of the adjacent ocean basins and overlying atmosphere around the Southern Ocean, thus helping to maintain zonal uniformity. This strong zonal flow must be maintained by the wind stress: topographic pressure drag is probably the dominant sink of momentum, with eddies affecting

the downward energy flux required to maintain the deep circulation (Bryden 1983). It is important to realize that while wind stress is not explicitly included in our model, its influence is accounted for through the assumption of zonal uniformity in the Southern Ocean.

We must now deal with the meridional exchange within the Southern Ocean and between the Southern Ocean and the two adjoining basins. Within the Southern Ocean there is clearly no geostrophic contribution to the zonally averaged overturning, except near the bottom, where topographic barriers can result in a nonzero zonally averaged pressure gradient. Consequently, north–south property gradients tend to be relatively strong within this region, and it is tempting to resolve this structure. However, in the interest of simplicity, we have modeled the Southern Ocean region by a single cell in the north–south direction. To test the influence of this idealization, additional experiments were performed with higher meridional resolution and $\epsilon = 0.0001$ within the Southern Ocean. As expected, the lack of an east–west pressure gradient greatly reduces the meridional flow in this region, but the influence is primarily localized and the global circulation is not significantly altered. More important, sensitivity to anomalous freshwater fluxes as well as the transient behavior during circulation changes are not influenced by increasing the meridional resolution of the model in the Southern Ocean.

It remains to consider exchange with the adjoining basins to the north. At the connecting boundaries with these regions, zonal barriers do exist and an east–west pressure difference can be maintained. To estimate the exchange across these sections, the average east–west pressure gradient is calculated by (1), and the resulting (nearly geostrophic) meridional velocity, together with horizontal diffusion, determines the meridional exchange between the northern basins and the zonally uniform Southern Ocean. Once these exchanges are calculated, vertical velocities within the Southern Ocean follow by continuity, and temperature and salinity evolve according to the usual advection–diffusion equations, with convection removing unstable density structures.

The numerical scheme used is the same as that in Part I. Fluxes across cell boundaries are estimated using the method of Fiadeiro and Veronis (1977), and forward time differencing is applied. The calculations discussed here are performed on grids with a total of either 15 or 31 cells in the meridional direction and either 10 or 20 cells in the vertical and $K_H = 10^3$ m^2 s^{-1}. For the coarser vertical resolution we will use $K_V = 0.4 \times 10^{-4}$ m^2 s^{-1} and $\tau_{H,S} = 100$ days, while for 20 vertical cells we select $K_V = 0.8 \times 10^{-4}$ m^2 s^{-1} and $\tau_{H,S} = 50$ days. A comparison of results obtained on the different grids is presented in the Appendix.

To obtain a steady-state circulation the standard procedure of ocean spinup is applied. Integration starts from an ocean at rest with uniform temperature $T = 7$°C and salinity $S = 35$ ppt. The circulation is set up by thermal and haline surface forcing. At the ocean surface T and S are relaxed to specified values T^* and S^* on a time scale $\tau_H = \tau_S = 100$ days. The following analytic forms are used initially:

$$T^*(s) = (1 + \cos(\pi s)) \times 12.5\text{°C} \quad (2a)$$

$$S^*(s) = (36 + \cos(\pi s)) \times \text{ppt}. \quad (2b)$$

Once a steady state under restoring boundary conditions is reached, the vertical salt flux is diagnosed, and further integrations are carried out under mixed boundary conditions: surface temperatures are still relaxed to (2a), while the salt flux is kept constant.

3. Global thermohaline circulation under symmetric salinity forcing

Here, temperature and salinity are restored to symmetric forcing fields, i.e., Pacific and Atlantic latitudes have identical restoring values given by (2). Figure 1a shows the meridional overturning streamfunction after 1000 years of spinup under restoring boundary conditions using the coarse 15 × 10 grid. The resulting thermohaline circulation consists of two cells in each

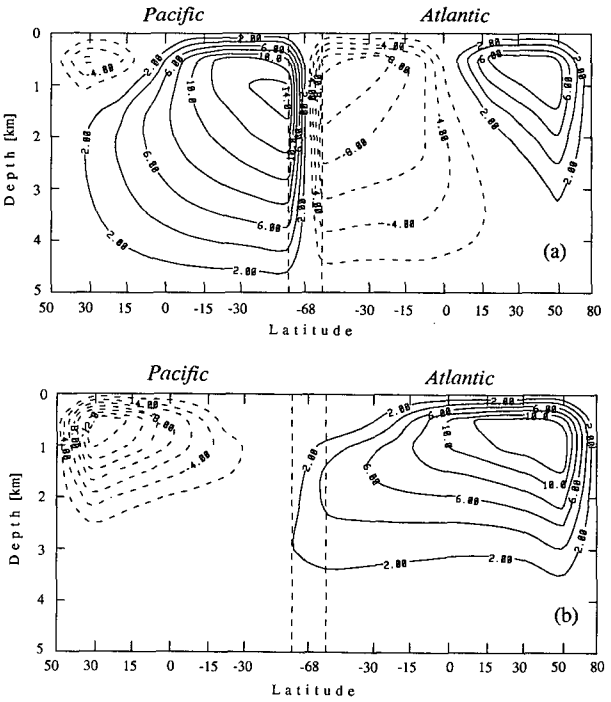

FIG. 1. Contours of the meridional overturning streamfunction in Sv (1 Sv = 10^6 m^3 s^{-1}) in the Pacific–Atlantic basin system. The Pacific extends from 50°N (left) to 55°S, where it joins the Atlantic basin extending to 80°N (right). Interbasin exchange occurs through the Southern Ocean, located within the two vertical dashed lines. The steady state under symmetric temperature and salinity restoring boundary condition (a) is unstable upon a switch to mixed boundary conditions and undergoes a transition to the final steady state (b).

ocean basin. Deep water is formed primarily in the Southern Ocean; intermediate water is formed in the North Atlantic and shallow overturning occurs in the North Pacific. There is very little mass exchange between the Pacific and Atlantic, and the flow shows the structure of two independent basins that are individually forced. The asymmetries between Pacific and Atlantic are primarily due to the fact that the Pacific basin only extends to 50°N.

The salt flux in both basins was diagnosed from this state, the boundary condition was switched to the mixed type, and a 0.5-ppt positive salinity anomaly was added to the surface layer of the Atlantic north of 32°N. As expected, the circulation is not stable, and after 1000 years the Southern Hemisphere cells in both basins have disappeared. The final steady state shows a one-cell circulation with deep-water formation in the northern latitudes of both basins (Fig. 1b). Interocean exchange did occur during the transient adjustment, but in the final equilibrium it has almost ceased, resulting in nearly independent thermohaline circulations in the two basins. This experiment shows that the geometrical asymmetry is not sufficient to produce a steady interocean exchange of water in this model. Under symmetric forcing, the system evolves to a state in which the interaction between the two basins is minimal.

4. Global thermohaline circulation under realistic salinity forcing

In this section steady-state circulations under restoring and mixed boundary conditions are obtained. The restoring profiles of T^* and S^* are given by (2a), and

$$S^*(s) = \left(35 + \cos(\pi s) + \frac{s_P - s_A}{s_P + s_A} + \begin{cases} +\Delta S \dfrac{s - s_{0A}}{s_P + s_A} \cdot \text{ppt}, & \text{Atlantic} \\ -\Delta S \dfrac{s - s_{0P}}{s_P + s_A} \cdot \text{ppt}, & \text{Pacific} \end{cases}\right), \quad (3)$$

where s_{0A}, s_{0P}, s_{1A}, and s_{1P} are the sines of the latitudes of the southern and northern extents of Atlantic and Pacific basins, respectively, and $s_P = s_{1P} - s_{0P}$, $s_A = s_{1A} - s_{0A}$. Superposed on the restoring salinity given by (2) is therefore a linear variation with an increase of about ΔS·ppt from the North Pacific through the Southern Ocean to the North Atlantic. We select $\Delta S = 2$ corresponding to realistic conditions and use the coarse 15 × 10 grid, unless stated otherwise. Due to the asymmetric salt forcing (3), the ocean spinup takes much longer to reach steady state. Since the vertical surface heat and salt fluxes integrated over both basins must vanish for a steady state, these quantities are useful indicators of deviations from equilibrium. After 7000 years of spinup under restoring boundary conditions, the integrated salt flux was four orders of magnitude smaller than typical values in each basin.

Figure 2 displays the meridional overturning streamfunction in the two ocean basins after 7000 years under restoring boundary conditions (2a) and (3). The state is steady, and deep water is formed at a rate of 16 Sv *in the North Atlantic only.* The Atlantic bottom water flows south, and about 7 Sv are exported into the Pacific. The rest is upwelling in the Atlantic and joins the thermocline return flow from the Pacific. In the Pacific about 10 Sv are upwelling, the main part of which originates from Atlantic bottom water. About 7 Sv are returned to the Atlantic as a shallow flow through the Southern Ocean (delineated by vertical dashes). Two weak and shallow cells in the South Atlantic and the North Pacific are also observed. From the state in Fig. 2 the salinity flux in both basins is diagnosed and used for further integration under mixed boundary conditions. When the integration is continued with no other changes, only small adjustments occur in the salinity field. While the effect is small, the fact that the system undergoes some change and evolves to a new equilibrium under mixed boundary conditions allows us to conclude that this state is *stable* against small perturbations. Sensitivity of this state to grid resolution is discussed in the Appendix.

To study the influence of the northward extension of the Atlantic basin, two additional spinup runs under restoring boundary conditions (2a) and (3) with $\Delta S = -2$ and $\Delta S = -4$ are performed; note that here the Atlantic is fresher than the Pacific. In the former case, $\Delta S = -2$, the circulation is similar to Fig. 1a, except that North Atlantic deep-water formation is shallow and sinking in the North Pacific reaches about 3000 m. No interocean flow is observed. Upon switching to mixed boundary conditions, this state is again unstable, and the new equilibrium state is similar to Fig. 1b.

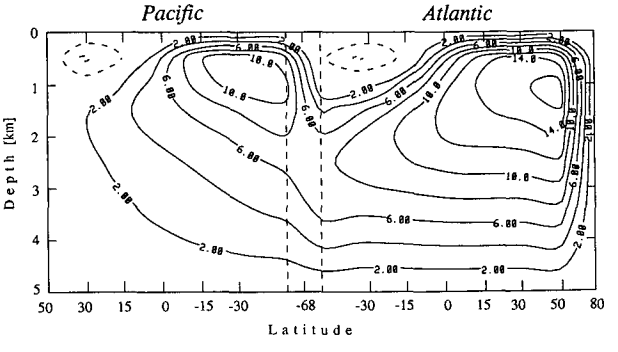

FIG. 2. Under restoring boundary conditions using realistic sea surface salinity, a global thermohaline circulation results. The steady state on the 15 × 10 grid, evolving from 7000 years of spinup, shows deep-water formation only in the North Atlantic, part of which is returned to form intermediate South Atlantic water. The rest spreads into the Pacific, where it upwells. Thermocline flow is to the south in the Pacific and to the north in the Atlantic.

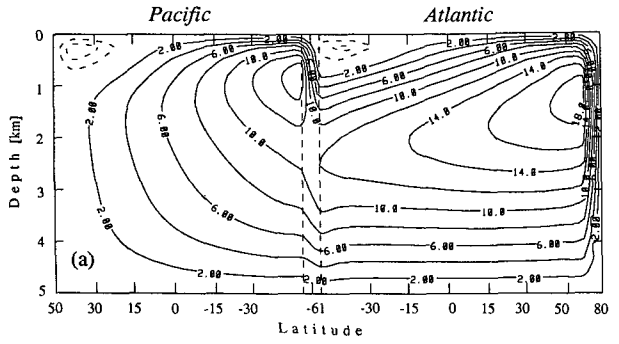

FIG. 3a. Meridional overturning streamfunction of the steady state at t = 8000 yr under mixed boundary conditions on the 31 × 20 grid with $K_V = 0.8 \times 10^{-4}$ m^2 s^{-1} and $\tau_H = \tau_S$ = 50 days. The negative contour interval is 1 Sv.

Only for the large salinity contrast, $\Delta S = -4$, does a reversed conveyor belt develop. Therefore, in this model the present geographical extension of the Pacific and Atlantic basins favors the conveyor belt circulation as shown in Fig. 2 but is not the cause of its maintenance. The latter point will be discussed below.

The temperature and salinity fields of the flow are now examined for a run with realistic salinity and temperature forcing. Restoring surface salinity is given by (3), and for the restoring surface temperature we select

$$T^*(s) = 14.5 + 12.5 \cos\left[\frac{\pi}{2} s(1 + |s|)\right] \text{ [°C]}, \quad (4)$$

which is a good approximation to the data of Levitus (1982). The model is spun up under restoring boundary conditions for 6000 years on the 31 × 20 grid using

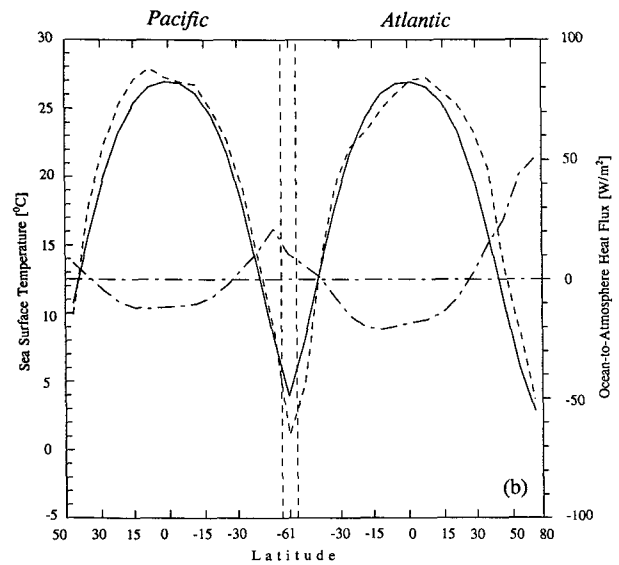

FIG. 3b. Sea surface temperature (solid), Levitus (1982) zonal averages (dashed), and ocean-atmosphere heat flux in W m^{-2} (dash-dotted) of the steady state of Fig. 3a.

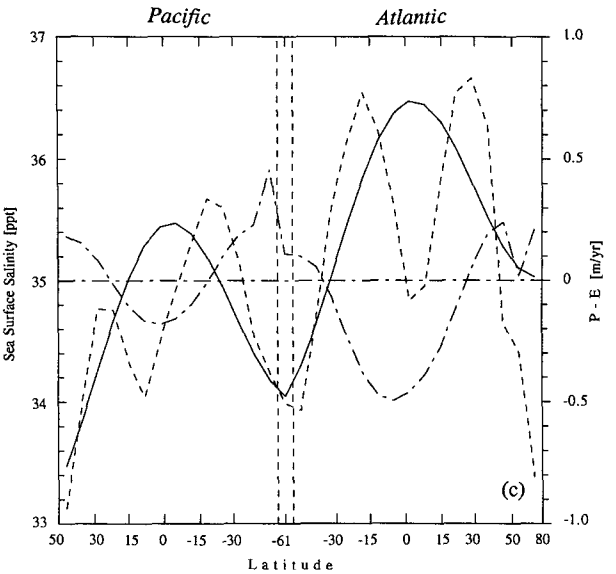

FIG. 3c. Sea surface salintity in ppt (solid), Levitus (1982) zonal averages (dashed), and P–E in m yr^{-1} (dash–dotted) of the steady state of Fig. 3a.

$K_V = 0.8 \times 10^{-4}$ m^2 s^{-1} and $\tau_S = \tau_H$ = 50 days. From this steady state the integration continues for 2000 years under mixed boundary conditions. The meridional overturning streamfunction at t = 8000 yr is shown in Fig. 3a. Deep-water formation occurs only in the North Atlantic at a rate of 19 Sv; 11 Sv flows as a deep current into the Pacific basin where it upwells over a broad

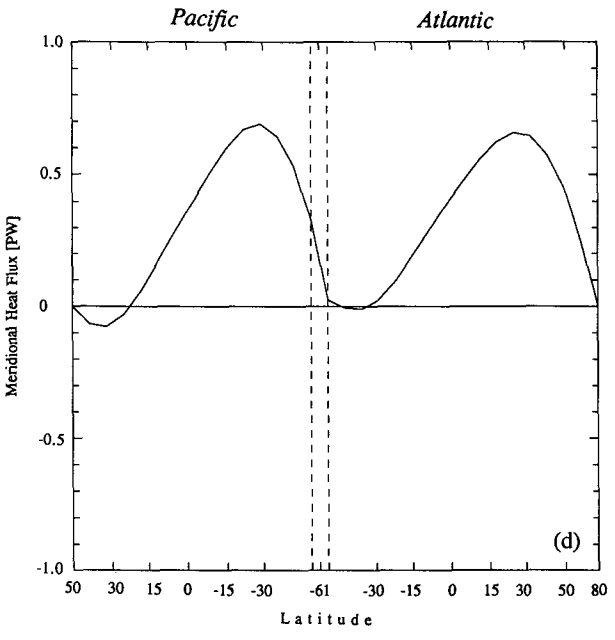

FIG. 3d. Meridional heat transport in PW (1 PW = 10^{15} W) integrated over the respective basin for the state of Fig. 3a. Heat is transported mainly to the south in the Pacific and to the north in the Atlantic.

region. Intermediate water is formed in the North Pacific (2.6 Sv) and in the Southern Ocean region (15 Sv), part of which (10 Sv) flows into the South Atlantic.

Figure 3b gives the latitude profiles of sea surface temperature (model and Levitus data) and the vertical ocean–atmosphere heat flux in watts per square meter. The model ocean temperature varies from 10.7°C (2.9°C) in the North Pacific (North Atlantic) to 27°C at the equator and falls to 4°C in the Antarctic Circumpolar Current region. The ocean receives energy at rates of 12 and 20 W m^{-2} in the equatorial regions of the Pacific and Atlantic, respectively. Most of the heat is released in the North Atlantic at an average of 30 W m^{-2} and at less than half this rate in the South Pacific.

Sea surface salinity (model and Levitus data) and the vertical salt flux are given in Fig. 3c as functions of latitude. Maximum salinities occur at the equator with 35.5 ppt in the Pacific and 36.5 ppt in the Atlantic; the North Pacific is fresh at 33.5 ppt compared to the North Atlantic at 35.0 ppt. The salt flux can be converted to P–E rates; the model shows a negative salt flux due to evaporation excess in the equatorial regions with 0.18 m yr^{-1} and 0.49 m yr^{-1} in the Pacific and Atlantic, respectively. The basin integral over the Atlantic indicates a *net evaporation excess* of 0.13 m yr^{-1} (0.06 m yr^{-1} and 0.21 m yr^{-1} over the North and South Atlantic, respectively), which in turn is compensated by a *net precipitation excess* over the Pacific. Baumgartner and Reichel (1975) give an observed value of 0.18 m yr^{-1} (0.12 m yr^{-1} and 0.24 m yr^{-1} over the North and South Atlantic, respectively). Considering the large uncertainties of these estimates, the model successfully reproduces the observed water transport through the atmosphere from the Atlantic to the Pacific. More details on the hydrological cycle are given below.

The Atlantic heat flux (Fig. 3d) is mainly northward with a maximum of 0.66 PW (0.41 PW across the equator). The Pacific, on the other hand, has a heat transport to the south peaking at 0.69 PW (0.37 PW across the equator). Although a substantial interocean mass flux is evident from Fig. 3a, there is very little exchange of heat between the basins.

Let us now compare the model results with the observed zonal averages of Levitus (1982). Figure 4 presents the model estimate of the latitude–depth temperature field of the Pacific and the corresponding observed field. Note that here and in the following figures the latitude scales are different, and no comparison can be made south of 55°S; as mentioned earlier, the present model makes no attempt to resolve the detailed water mass structures within the Southern Ocean.

The model shows the observed stratification and the well-mixed regions of the upper 1000 m of the South Pacific. As expected, the equatorial doming due to Ekman pumping is not present in the model. The salinity fields are given in Fig. 5. Near the equator the model and observed salinities decrease with depth over the upper 600 m, below which there is intermediate water exhibiting very weak salinity gradients. From both the north and the south, tongues of freshwater intrude equatorward between about 600 m and 1000 m. The deep ocean is uniformly stratified with only a very weak latitude dependence showing doming in the equatorial regions. All these features are in general agreement with the observations.

The temperature field of the Atlantic (Fig. 6) is similar to that of the Pacific, showing a vertically stratified structure. Again, the equatorial doming is not produced by this purely buoyancy-driven model. Strong vertical mixing is visible in the North Atlantic where deep water is formed. This is in general agreement with the data. The deep ocean does not show the cooler waters reaching the ocean bottom from the Southern Ocean. Figure 7 gives the model (a) and Levitus (b) salinity fields of the Atlantic. The model again reproduces the inverse stratification of the upper ocean at low latitudes. A prominent observed feature of the Atlantic is the intrusion of fresh thermocline water from the Southern Ocean, beneath which saltier water penetrates from the north to form a wedge of saltwater in the deep ocean. Both structures are present in the model although the intrusion of Antarctic intermediate water proceeds too far north.

In spite of the various idealizations, both temperature and salinity fields of the Atlantic and Pacific are reproduced fairly realistically. In particular, the model is able to give the gross water mass structures for both the Pacific and the Atlantic. These are very different in the two ocean basins. In the Pacific the low-latitude intermediate water shows a well-mixed region that is enclosed by freshwater tongues from the north and south. The corresponding Atlantic water, on the other hand, is dominated by a freshwater wedge emanating from the Southern Ocean and overlying a wedge of saltwater from the north. Both phenomena are present in the model fields, which suggests that the observed T and S structures in the two ocean basins are direct evidence for the presence of interocean thermohaline flow. The largest differences between the model and observed fields are, as expected, in the Southern Ocean, the meridional structure of which the model makes no attempt to resolve.

Atmospheric freshwater transport is essential to maintain the global thermohaline circulation. This is confirmed by an experiment on the 31×10 grid starting from the steady-state conveyor belt (corresponding to Fig. 3a) and reducing the Atlantic–Pacific freshwater transport by 80%. Time series of some characteristic variables are given in Fig. 8. Maximum and minimum Atlantic overturning and the net surface heat flux over both basins are shown in Fig. 8a. The negative cell in the southern Atlantic increases in strength for about 500 years with relatively minor adjustments of the water mass properties (see Fig. 8b), until the two Atlantic

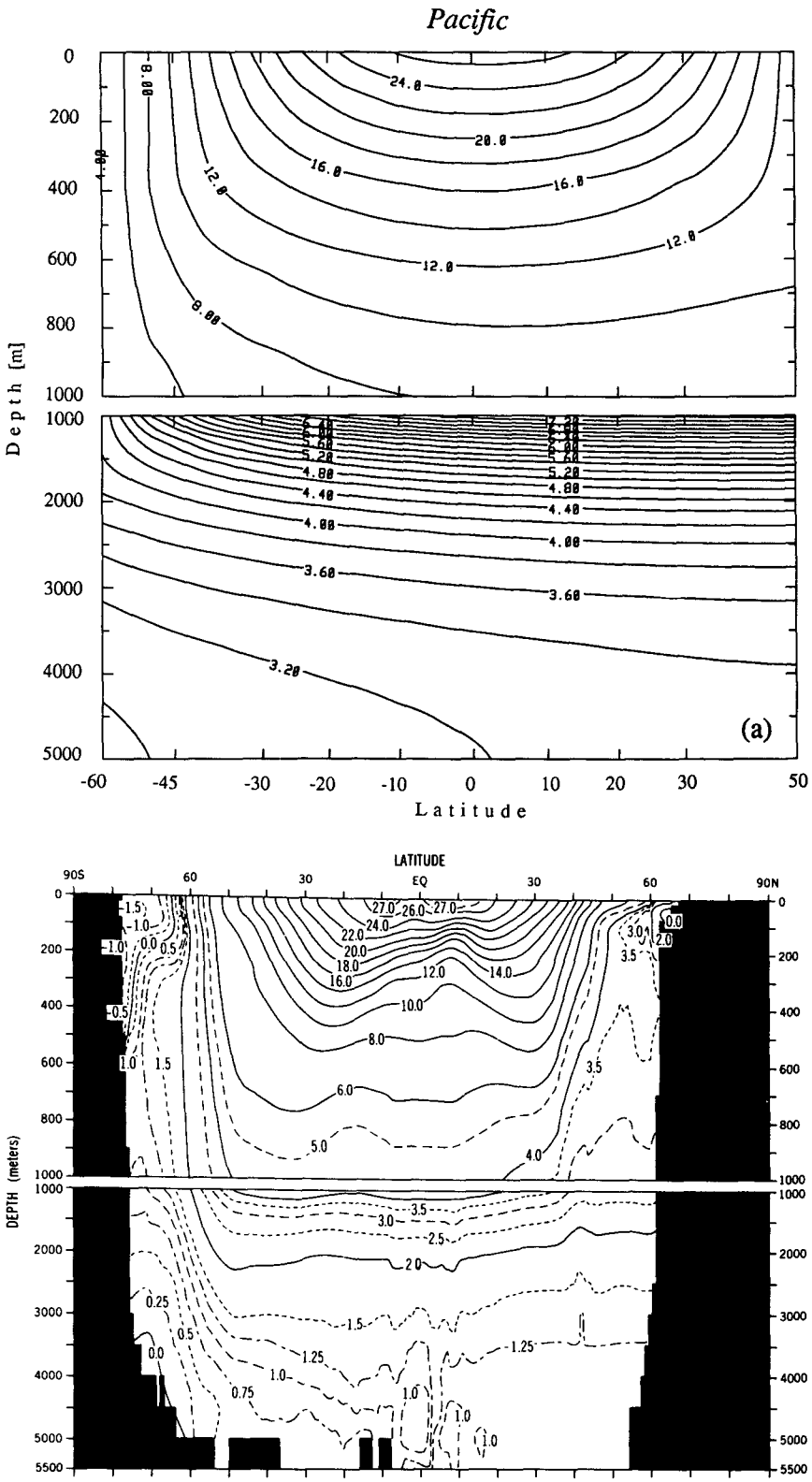

FIG. 4. Comparison of (a) the zonally averaged temperature field in the Pacific for the steady state of Fig. 3a with (b) the observed temperature from Levitus (1982).

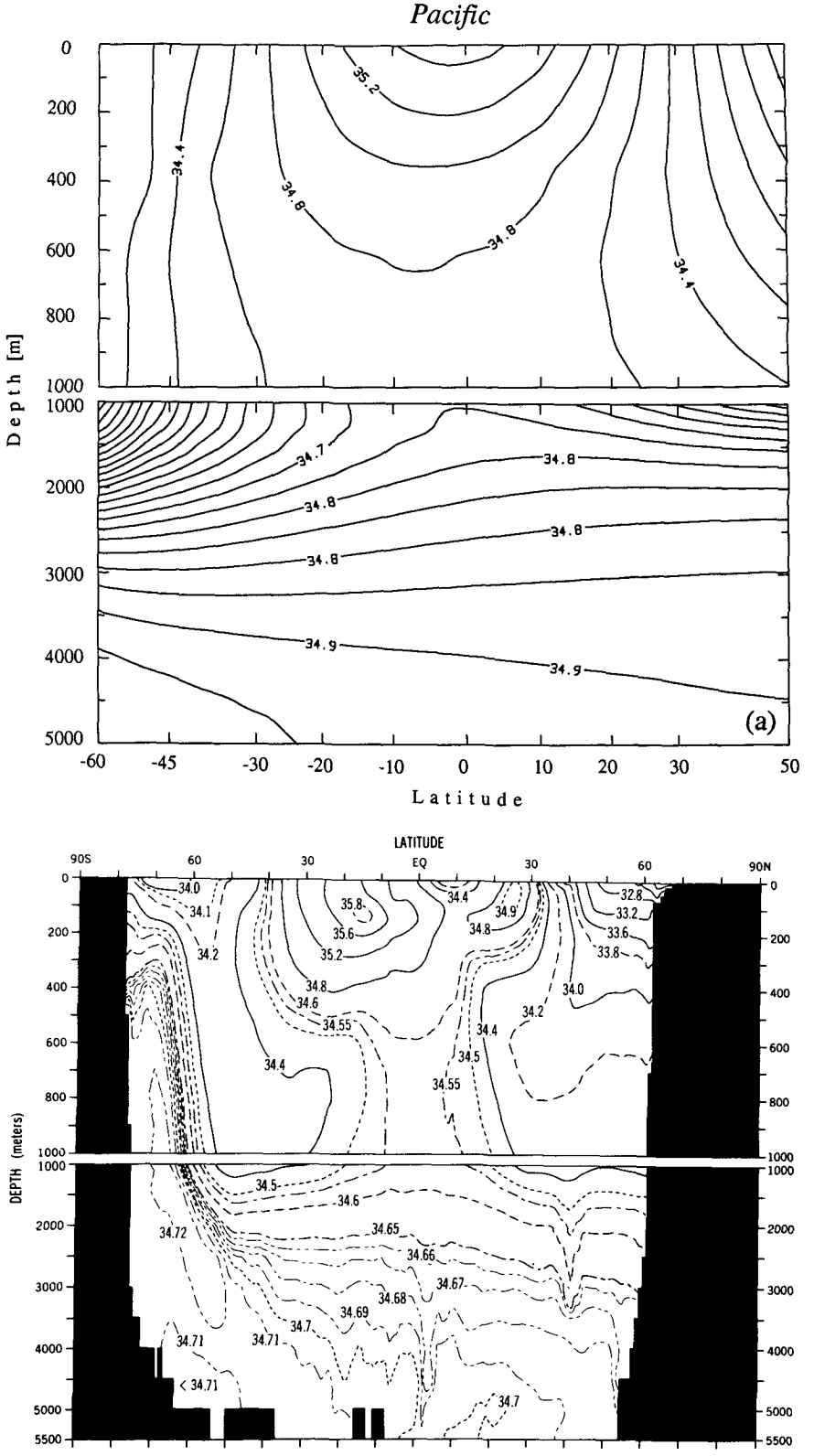

FIG. 5. Comparison of (a) the zonally averaged salinity field in the Pacific for the steady state of Fig. 3a with (b) Levitus (1982).

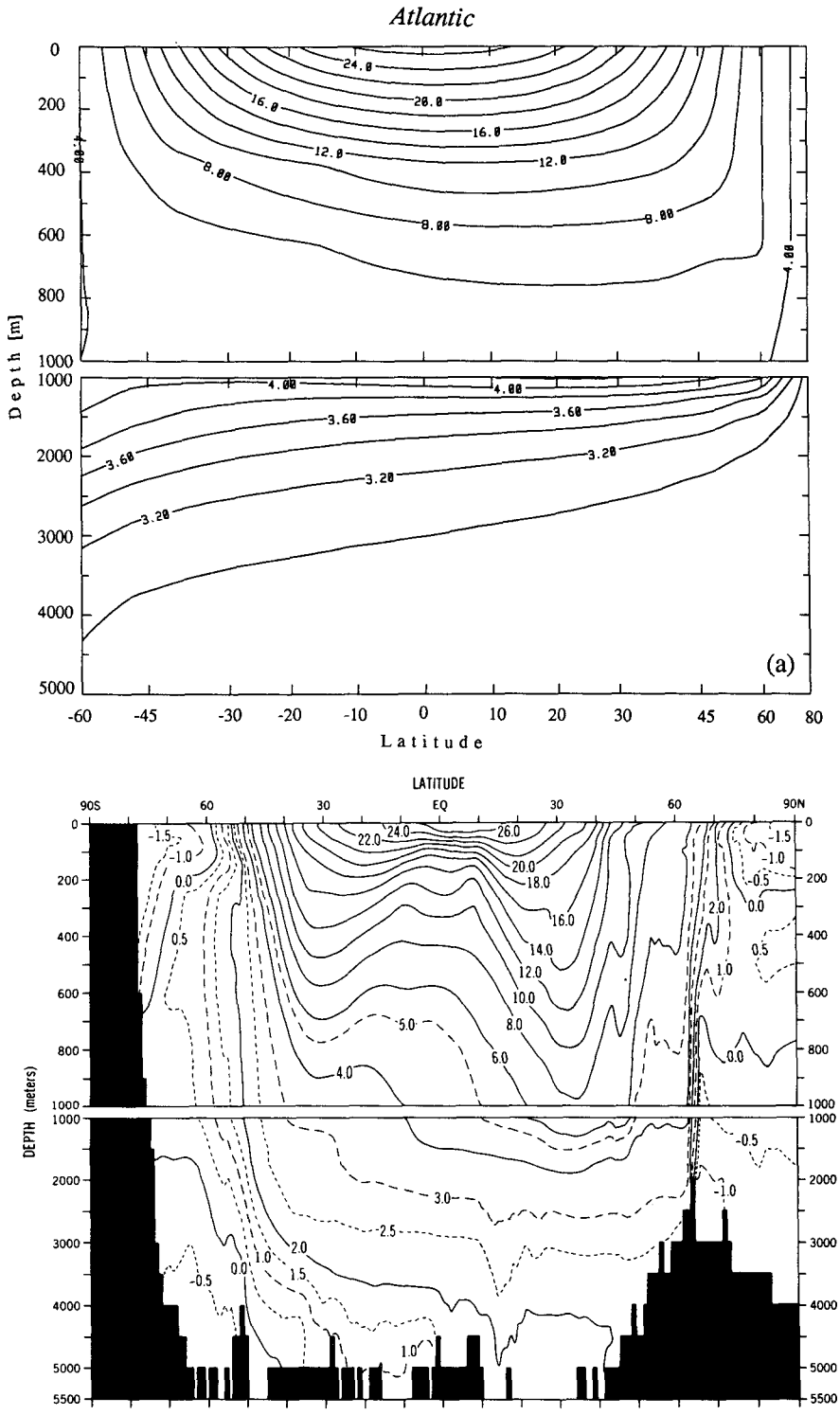

FIG. 6. Comparison of (a) the zonally averaged temperature field in the Atlantic for the steady state in Fig. 3a with (b) Levitus (1982).

cells have about equal strength. At this time instability of the two-cell circulation in the Atlantic occurs, and a relatively rapid transition accompanied by strong convective events is completed within the next 400 years. The positive cell disappears, and a steady state, which has one cell in each basin with deep-water for-

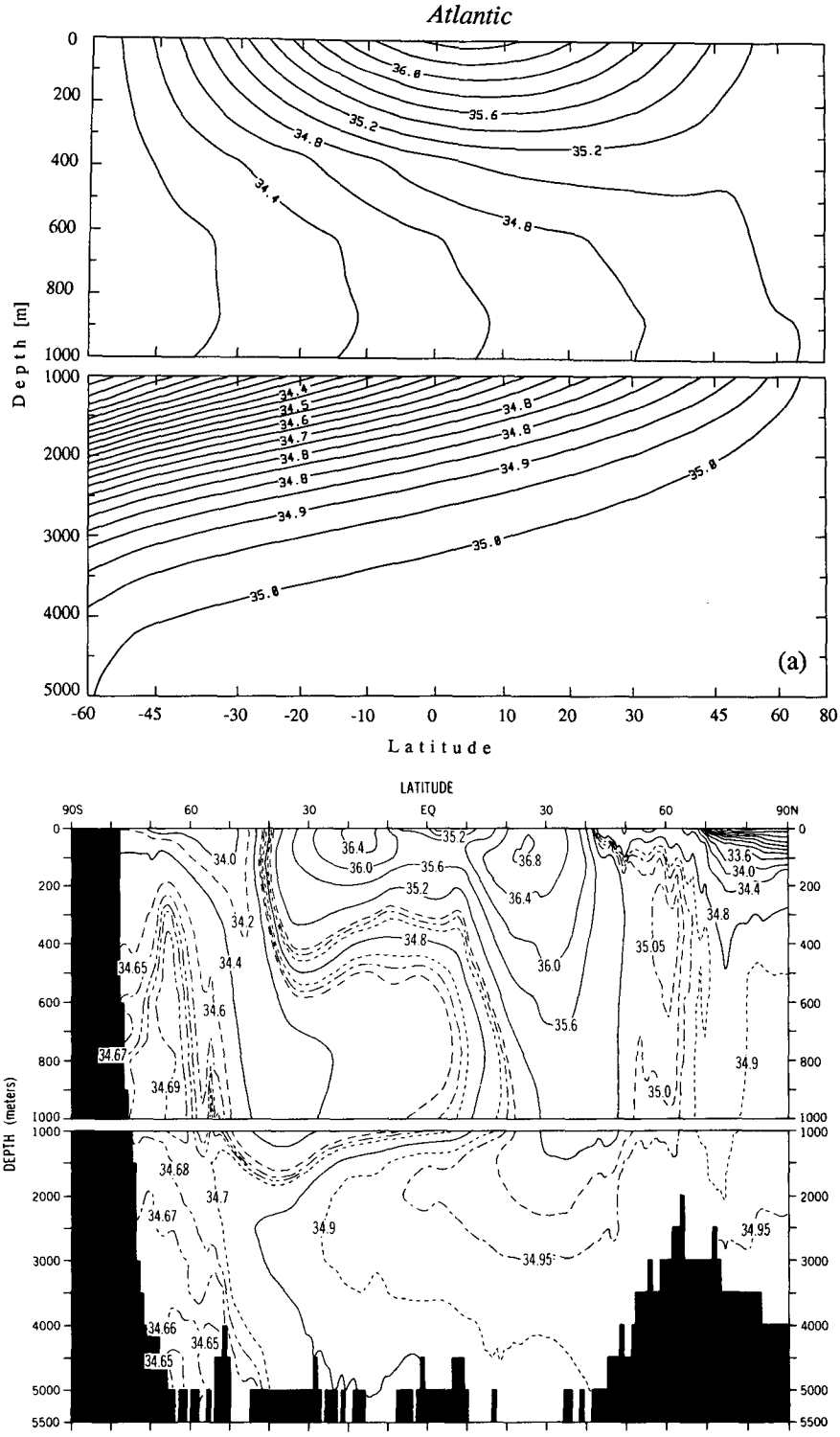

FIG. 7. Comparison of (a) the zonally averaged salinity field in the Atlantic for the steady state of Fig. 3a with (b) Levitus (1982).

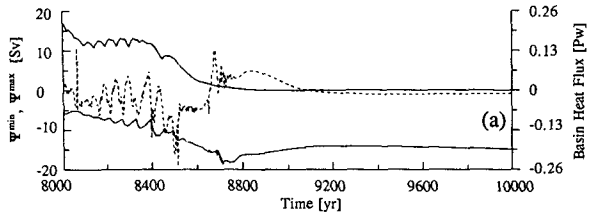

FIG. 8a. Time series of the maximum and minimum Atlantic overturning rates (solid) and the basin-integrated ocean–atmosphere heat flux in PW (dashed). Reduction of the atmospheric Atlantic–Pacific freshwater transport by 80% causes the destruction of the conveyor belt, and the circulation in the Atlantic reverses.

mation in the southern latitudes, results similar to Fig. 9a. The reduced freshwater exchange between the basins causes the mean Pacific surface salinity to increase only slightly (Fig. 8b, dashed). For the first few hundred years the excess freshwater in the surface of the Atlantic is removed to the deep ocean. However, this reduces the meridional density gradients that drive the deep positive cell in the North Atlantic. The cell weakens and ultimately collapses. Consequently, the mean surface salinity in the Atlantic drops by 2.6 ppt. During the transition from the conveyor belt to the new equilibrium state, both deep basins receive heat and warm up by about 0.4°C (Fig. 8b, solid). In the new steady state the Atlantic is fresher than the Pacific.

In summary, the present two-dimensional ocean model reproduces the global thermohaline circulation proposed by Gordon (1986) and is capable of modeling the main structure of the latitude–depth distribution of both temperature and salinity. The importance of atmospheric water vapor transport for the maintenance of this interocean exchange of water is demonstrated.

5. Stability of the Pacific–Atlantic interocean circulation

It has often been argued in recent years that the ocean circulation might have more than one stable mode of operation. Transitions between different equilibria can be triggered by freshwater flux anomalies, which occur naturally during the termination of ice ages. The most recent termination, the transition into the present Holocene started about 14 000 years ago, caused the complete melting of the Laurentide and several other, smaller continental ice sheets in the Northern Hemisphere. Denton and Hughes (1981) estimate that 30 $\times 10^6$ km^3 melted during a period of about 8000 years. We assume, taking the simplest possible scenario, that this volume was released at a constant rate of about 0.12 Sv into the Atlantic. Broecker et al. (1985) suggest that the river discharge changed from the Mississippi, at the earlier stages of the melting, to the St. Lawrence later. Several other melting scenarios have been proposed, and Fairbanks (1989) reports a recent reconstruction.

To test the influence of such freshwater additions, two experiments are conducted on the 31 × 10 grid with $K_V = 0.4 \times 10^{-4}$ m^2 s^{-1}. The model is spun up from rest under the restoring boundary conditions (2a) and (3). At t = 7000 yr mixed conditions are applied; the perturbation experiments start at t = 8000 yr from the conveyor belt circulation. A salt flux anomaly corresponding to a freshwater flux of 0.12 Sv for Expt. I is applied at 15°N for 4000 years and then moved to 45°N for another 4000 years to model the change in discharge location. At t = 16000 yr the anomaly is shut off, and the system was integrated until t = 27 000 yr. Experiment II tests the same scenario for half the anomaly, i.e., 0.06 Sv.

Figure 9 displays the meridional overturning at t = 12 000 yr for Expts. I (a) and II (b). The realistic anomaly of Expt. I causes a breakdown of the global conveyor belt and a *complete reversal* of the North Atlantic thermohaline circulation. Deep water is now formed in the South Atlantic, and the North Atlantic shows upwelling. The flow in the Pacific, on the other hand, has not changed much, except that sinking in the Southern Ocean now reaches deeper depths. Interocean exchange has stopped, and the two basins exhibit rather independent fields. This state was already established 600 years after the anomaly was initiated. Only minor adjustments occur when the flux anomaly is moved north. Once the flux anomaly is shut off, the North Pacific cell decreases in strength, but the final steady state obtained at t = 27 000 yr (10 000 years after the anomaly was switched off) has still one cell in each basin with downwelling in the Southern Ocean. When only half the anomaly is applied to the conveyor belt, the shallow South Atlantic cell is intensified, but the global thermohaline circulation remains in operation (Fig. 9b). After the anomaly is shut off, the system returns to the original equilibrium state.

In Fig. 10 we present the evolution of some characteristics in both basins for the first 2000 years of Expt. I. The anomalous freshwater input decreases deep-water formation in the Atlantic steadily, while the negative cell in the South Atlantic is increasing in strength. After about 400 years the Atlantic surface salinity decreases, indicating that the freshwater is no longer exported to the deep ocean. The new equilibrium state shows again

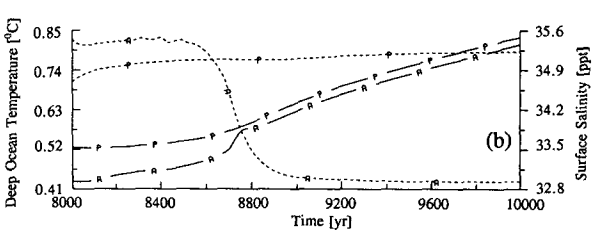

FIG. 8b. Time series of the mean deep-ocean temperature (>3000 m, solid) and mean surface salinity (dashed) in the Atlantic and Pacific.

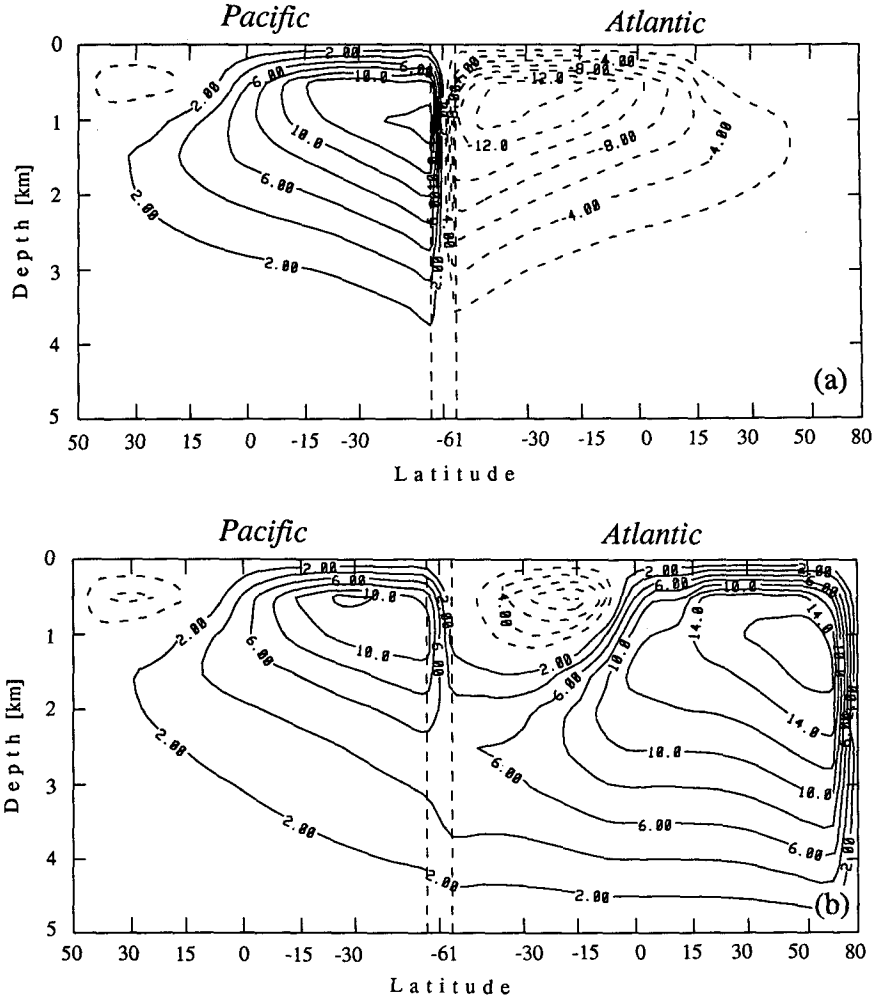

FIG. 9. The steady-state global thermohaline circulation under mixed boundary conditions after 4000 years of the deglaciation experiments. The conveyor belt circulation is perturbed by an Atlantic freshwater flux anomaly of 0.12 Sv for (a) and 0.06 Sv for (b), applied at 15°N for 4000 years. The strong anomaly causes the Atlantic circulation to reverse (a), while the weak anomaly only causes minor adjustments to the conveyor belt (b).

a warmer deep ocean. Qualitatively, the transition evolved like that in Fig. 8, suggesting that local freshwater anomalies and global changes to the hydrological cycle can have similar effects on the global thermohaline circulation.

It should be noted that there are differences between our results and those of Maier-Reimer and Mikolajewicz (1989) in their three-dimensional Hamburg OGCM. First, they find that the thermohaline circulation collapses within the first 100 years whereas here, in Expt. I, after 400 years the conveyor belt has disappeared and the Atlantic circulation consists of two cells of about equal strength. The response time in the two-dimensional model can be reduced to less than 200 years by placing the flux anomaly directly into the region of deep-water formation. In the three-dimensional model the freshwater is efficiently carried northward by the western boundary current, providing a mechanism for a faster response time. Second, the two-dimensional model appears to be less sensitive to an anomalous salinity flux, as shown in Expt. II. In comparison, the Atlantic thermohaline circulation of the Hamburg OGCM can be shut off by a small anomaly of only 0.01 Sv. As Birchfield et al. (1990) note with regard to the GCM results of Bryan (1986) and Manabe and Stouffer (1988), it appears possible that the steady state of the Hamburg OGCM may have been close to an unstable equilibrium point. Indeed, additional experiments have shown that reducing horizontal diffusivity can significantly increase sensitivity to anomalous freshwater fluxes in the two-dimensional model. Also, a more realistic surface forcing using the zonally averaged temperatures and salinities of Levitus (1982) helps increase sensitivity significantly. It is also im-

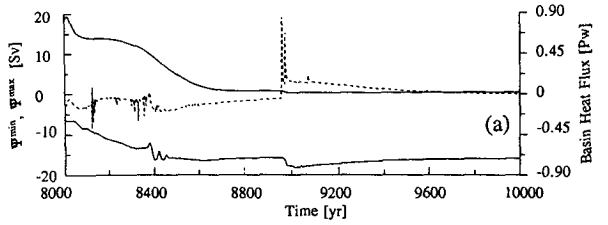

FIG. 10a. Time series of the maximum and minimum Atlantic overturning (solid) and the basin-integrated vertical heat flux (dashed) for the first 2000 years of the deglaciation Expt. I. A steady inflow of 0.12 Sv of freshwater into the Atlantic causes a breakdown of the conveyor belt within a few hundred years.

portant to note that the two-dimensional model probably overestimates the influence of the near-surface salinity contrast between the Atlantic and the Pacific and hence the stability of the conveyor belt, due to the use of rather coarse vertical resolution.

The two experiments demonstrate that the present model possesses two stable states of the coupled Pacific–Atlantic basin system under the same forcing. A realistic flux anomaly is capable of causing a transition from the state with interocean exchange to a state in which the thermohaline circulations of Pacific and Atlantic operate independently. The oceanic heat transport is dramatically different for the two states. Figure 11 compares the meridional heat transport of the initial steady state (solid), Expt. I (dashed), and Expt. II (dash–dotted) at t = 12 000 yr. In Expt. I the Atlantic heat flux is to the south with very little transport in the highest latitudes. In the Pacific, on the other hand, modifications are only minor. Experiment II shows changes only in the South Atlantic, where the heat flux is increased. Again, the Pacific flux is unaltered.

It is the vertical ocean–atmosphere heat flux from which we expect climatic changes that would be detected in proxy data. Table 1 shows the average vertical heat flux in the North Atlantic from 50° to 80°N (a), and in the North Pacific from 41° to 50°N (b). Changes in the North Pacific are too small to cause a detectable signal in any proxy record. However, in the Atlantic the heat flux reduces by 25 W m^{-2} for Expt. I and 3.3 W m^{-2} in Expt. II; the corresponding values in the Pacific do not exceed 0.7 W m^{-2}. To give a

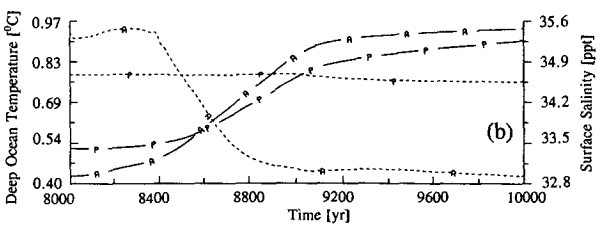

FIG. 10b. Time series of the mean deep-ocean temperature (>3000 m, solid) and mean surface salinity (dashed) in Atlantic and Pacific for the first 2000 years of Expt. I.

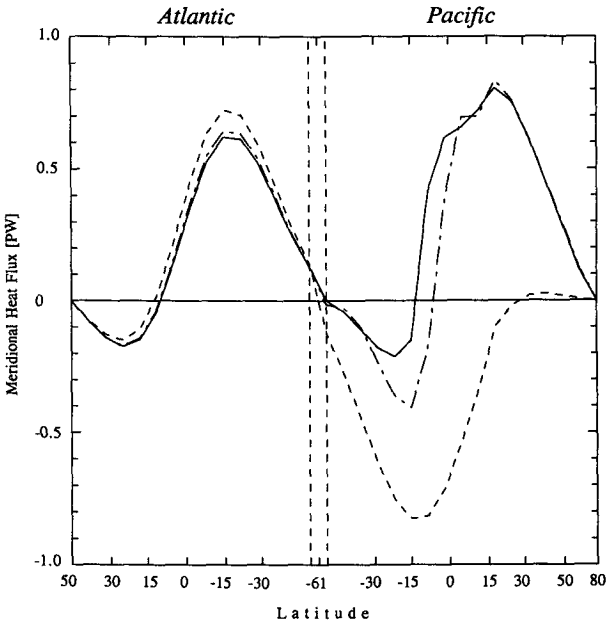

FIG. 11. Meridional heat transport in PW for the steady-state conveyor belt (solid), the new equilibrium state for Expt. I (dashed) as given in Fig. 9a and the perturbed conveyor belt for Expt. II (dash–dotted) of Fig. 9b.

rough upper estimate for the associated surface air temperature changes, we use a greybody radiation estimate, $\delta Q = 4\sigma e T^3 \delta T$, with a mean emissivity of $e = 0.6$ and high-latitude temperature $T = 4$°C, to obtain temperature changes of order −9°C (Expt. I) and −1°C (Expt. II) in the Atlantic; in the Pacific changes are less than 0.2°C. Both Atlantic signals could, if present, be observed in oxygen isotope records. The picture here is consistent with Broecker et al. (1985) who find the Younger Dryas signal only in locations that are under the influence of the North Atlantic (Europe, Greenland, and the Canadian maritime), but not where changes in the north Pacific would have a major effect on the climate (central and western North America).

6. Conclusions

The model developed in Part I was extended to simulate a possible global thermohaline circulation, which

TABLE 1. Average vertical heat flux (W m^{-2}) in the North Atlantic between 50°N and 80°N and in the north Pacific between 41°N and 50°N.

Freshwater anomaly		t (years) 8000	12 000	16 000	17 000
Expt. I 0.12 Sv	Atlantic	12.4	−12.6	−12.6	−12.7
	Pacific	8.3	7.9	7.8	7.6
Expt. II 0.06 Sv	Atlantic	12.4	9.9	8.7	11.4
	Pacific	8.3	8.3	8.4	8.3

connects the Pacific and Atlantic and allows for interocean exchange of mass, heat, and salt. The state obtained under restoring boundary conditions with identical latitude profiles of salinity for both basins consists of a two-cell circulation in both Pacific and Atlantic. Atlantic deep-water formation is more pronounced due to the increased northward extent of this basin. The main deep-water production, however, is in the Southern Ocean. Upon a switch to mixed boundary conditions, the system shows a transition with strong interocean exchange of water. The final steady state is one with deep-water formation in both high northern latitudes and very little cross-basin flow.

The essential features of a global thermohaline circulation proposed by Gordon (1986) could be realized by restoring to an asymmetric surface salinity profile that is fresher in the Pacific; this corresponds to present-day conditions. Deep water is now formed only in the North Atlantic from where it spreads into the Pacific to upwell. The main features of the latitude–depth structure of temperature and salinity show fair agreement with the zonal averages by Levitus (1982). The state is stable under mixed boundary conditions. We have also shown that the present geographical extension of Pacific and Atlantic basins favors a conveyor belt circulation of this nature: it seems unlikely that the conveyor belt actually reverses direction as hypothesized by Broecker et al. (1985).

The global circulation is maintained by a net freshwater flux from the Atlantic to the Pacific through the atmosphere. If this flux is removed, the oceanic circulation changes on a comparatively short time scale (here about 600 years) to a state in which deep water is formed in both southern latitudes with very little interocean exchange. This emphasizes the key importance of the hydrological cycle in determining the thermohaline flow and hence the direction of the oceanic heat flux.

We analyzed the stability of this interocean flow by conducting a deglaciation experiment. The stable state under mixed boundary conditions was perturbed by a salt flux anomaly of 0.12 Sv and 0.06 Sv during 8000 years. The strong anomaly causes the Atlantic circulation to reverse completely within the first 600 years of the experiment, thereby inhibiting any interbasin flow. Eventually, the stable one-cell circulation is reached in each basin individually. However, the conveyor belt persisted for the weaker anomaly and exhibited decreased ocean–atmosphere heat fluxes in the North Atlantic. For both scenarios the Pacific thermohaline circulation did not change much; this is consistent with the spatial distribution of the Younger Dryas climate event (Broecker et al. 1985).

The deglaciation experiment also showed that the global thermohaline circulation is stable for small perturbations. However, a second stable state under identical surface forcing exists. In this state there is little interocean exchange, and the thermohaline circulations of Pacific and Atlantic basins operate independently. A transition is possible for salt flux anomalies exceeding a threshold value, which lies within present estimates of glacial meltwater fluxes at the last termination.

The present paper emphasizes the significance of the thermohaline circulation of the ocean for climate change. It is shown that multiple equilibria are realized under present-day forcing. The atmospheric part of the hydrological cycle (including runoff) plays a crucial role in maintaining the salinity contrast between the Atlantic and the Pacific and hence the global conveyor belt. The eventual goal is to incorporate two-dimensional models of the atmosphere and the cryosphere in order to obtain a realistic and yet inexpensive model suitable for paleoclimatic studies. This work is in progress (Stocker et al. 1991).

Acknowledgments. The fellowship 82.613.0.88 of the Swiss National Science Foundation awarded to TFS, professional development leave for DGW, and research grants from the Canadian Natural Sciences and Engineering Research Council and Atmospheric Environment Service awarded to L. A. Mysak made this study possible. TFS thanks Dr. E. P. Jones for the hospitality and support by a Canadian Panel on Energy Research and Development contract. We enjoyed discussions with Drs. L. A. Mysak and A. J. Weaver.

APPENDIX

Sensitivity to Grid Resolution and Vertical Diffusivity

Here we examine the dependence of the flow on the grid resolution. Vertical diffusivity and relaxation time scales are given in Table A1. Calculations are performed on three different grids with 15 (meridional) $\times$ 10 (vertical), 31 $\times$ 10, and 31 $\times$ 20 cells. Spinup under restoring boundary conditions, followed by a switch to mixed boundary conditions, is repeated independently for each grid resolution and qualitatively similar flows are obtained. The maximum transport does not vary much when the horizontal resolution is increased. However, with double the vertical resolution we get a significant reduction in the maximum transport (Table A1).

Part of this discrepancy can be directly related to the restoring surface boundary condition [Part I: Eqs. (11), (12a)]. As Δz is reduced, the relaxation time scale should also be reduced approximately in proportion. However, vertical diffusivity is also important. Because temperature is taken to vary linearly through the two uppermost grid cells, the influence of the surface boundary condition extends to greater depths for coarser vertical resolution. By doubling K_V and halving the relaxation time we obtain similar transports again.

The dependence of the meridional overturning on vertical diffusivity was also examined on the 31 $\times$ 10 grid (Table A1). By increasing K_V from 0.4 to 0.8 $\times 10^{-4}$ m^2 s^{-1}, the maximum transport was increased

TABLE A1. Comparison of maximum transport and meridional heat flux for different grid resolutions, vertical diffusivities, and relaxation time scales.

Grid	K_V (10^{-4} m^2 s^{-1})	$\tau_{H,S}$ (days)	North Atlantic overturning (Sv)	Maximum meridional heat flux (PW)	
				Atlantic (north)	Pacific (south)
15 × 10	0.4	100	16.9	0.81	0.63
31 × 10	0.4	100	17.0	0.74	0.60
31 × 10	0.8	100	20.2	0.92	0.78
31 × 20	0.4	100	11.9	0.41	0.40
31 × 20	0.8	50	17.2	0.59	0.62

by about 19%, in fair agreement with the 1/3-power law found by Bryan (1987).

Finally, we note an interesting phenomenon that occurs using the 31 × 10 grid. A remarkable periodic variability of the global thermohaline circulation is observed. The period is 38 yr, and once initiated the fluctuations persist throughout the 8000 years of integration with a peak-to-peak amplitude of 1.2 Sv or about 7%. Similar variability can be inferred for the climate-relevant meridional heat transport. Given the steady forcing, the variability is apparently a self-sustained oscillation. Therefore, even in this idealized ocean model, natural variability under mixed boundary conditions *does* occur, indicating again that the ocean is an active component of the climate system. A similar phenomenon of decadal variability was recently found by Weaver and Sarachik (1991) in their three-dimensional OGCM. The self-sustained oscillation is absent for doubled vertical diffusivity, and no fluctuation of the steady state is observed. A spurious numerical mode can be excluded as a cause of the variability in the previous run; one cycle of the oscillation is covered by more than 550 time steps. The result rather indicates that the vertical diffusivity is an important parameter that strongly influences the natural variability of the thermohaline circulation. Further work is in progress to elucidate the physical mechanisms and the time scales that are involved.

REFERENCES

Baumgartner, A., and E. Reichel, 1975: *The World Water Balance.* Elsevier, 179 pp.

Birchfield, G. E., H. Wang and M. Wyant, 1990: A bimodal climate response controlled by water vapour transport in a coupled ocean–atmosphere box model. *Paleoceanogr.*, **5**, 383–395.

Broecker, W. S., and G. H. Denton, 1989: The role of ocean–atmosphere reorganizations in glacial cycles. *Geochim. Cosmochim. Acta,* **53**, 2465–2501.

——, D. M. Peteet and D. Rind, 1985: Does the ocean–atmosphere system have more than one stable mode of operation? *Nature,* **315**, 21–26.

Bryan, F., 1986: High-latitude salinity effects and interhemispheric thermohaline circulations. *Nature,* **323**, 301–304.

——, 1987: Parameter sensitivity of primitive equation ocean general circulation models. *J. Phys. Oceanogr.*, **17**, 970–985.

Bryden, H. L., 1983: The Southern Ocean. *Eddies in Marine Science,* A. R. Robinson, Ed., Springer, 265–277.

Cox, M. D., 1989: An idealized model of the world ocean. Part I: The global-scale water masses. *J. Phys. Oceanogr.*, **19**, 1730–1752.

Denton, G. H., and T. J. Hughes, 1981: *The Last Great Ice Sheets.* Wiley, 484 pp.

Fairbanks, R. G., 1989: A 17 000-year glacio–eustatic sea level record: Influence of glacial melting rates on the Younger Dryas event and deep-ocean circulation. *Nature,* **342**, 637–642.

Fiadeiro, M. E., and G. Veronis, 1977: On weighted-mean schemes for the finite-difference approximation to the advection–diffusion equation. *Tellus,* **29**, 512–522.

Gordon, A. L., 1986: Interocean exchange of thermocline water. *J. Geophys. Res.*, **91**, 5037–5046.

Levitus, S., 1982: *Climatological Atlas of the World Ocean.* NOAA Prof. Paper, **13**, 173 pp.

Maier-Reimer, E., and U. Mikolajewicz, 1989: Experiments with an OGCM on the cause of the Younger Dryas. *Oceanography,* A. Ayala-Castañares, W. Wooster and A. Yáñez-Arancibia, Eds., UNAM Press, 87–100.

Manabe, S., and R. J. Stouffer, 1988: Two stable equilibria of a coupled ocean–atmosphere model. *J. Climate,* **1**, 841–866.

Marotzke, J., and J. Willebrand, 1991: Multiple equilibria of the global thermohaline circulation. *J. Phys. Oceanogr.*, in press.

——, P. Welander and J. Willebrand, 1988: Instability and multiple equilibria in a meridional-plane model of the thermohaline circulation. *Tellus,* **40A**, 162–172.

Stocker, T. F., D. G. Wright, and L. A. Mysak, 1991: A zonally averaged, coupled ocean–atmosphere model for paleoclimate studies. *J. Climate,* in press.

Stommel, H., 1961: Thermohaline convection with two stable regimes of flow. *Tellus,* **13**, 224–230.

Warren, B. A., 1981: Deep circulation of the world ocean. *Evolution of Physical Oceanography, Scientific Surveys in Honor of Henry Stommel,* B. A. Warren, and C. Wunsch, Eds., MIT Press, 6–41.

Weaver, A. J., and E. S. Sarachik, 1991: Evidence for decadal variability in an ocean general circulation model: An advective mechanism. *Atmos.–Ocean,* **29**, 197–231.

Wright, D. G., and T. F. Stocker, 1991: A zonally averaged model for the thermohaline circulation. Part I: Model development and flow dynamics. *J. Phys. Oceanogr.*, **21**, 1713–1724.